



The Extended Continental Crust West of Islas Marías (Mexico)

OPEN ACCESS

Edited by:

Pier Paolo Bruno,
University of Naples Federico II, Italy

Reviewed by:

Takeshi Sato,
Japan Meteorological Agency, Japan
Drew Eddy,
BHP Billiton, Australia

*Correspondence:

Diana Núñez
diana@sisvoc.mx

†ORCID:

Diana Núñez
orcid.org/0000-0003-0572-3905
Jorge A. Acosta-Hernández
orcid.org/0000-0002-6709-3577
Felipe de J. Escalona-Alcázar
orcid.org/0000-0002-4066-6160
Simone Pilia
orcid.org/0000-0002-3125-042X
Francisco J. Núñez-Cornú
orcid.org/0000-0003-1515-1349
Diego Córdoba
orcid.org/0000-0003-1106-3632

Specialty section:

This article was submitted to
Solid Earth Geophysics,
a section of the journal
Frontiers in Earth Science

Received: 09 February 2021

Accepted: 27 August 2021

Published: 23 September 2021

Citation:

Núñez D, Acosta-Hernández JA,
Escalona-Alcázar FdeJ, Pilia S,
Núñez-Cornú FJ and Córdoba D
(2021) The Extended Continental Crust
West of Islas Marías (Mexico).
Front. Earth Sci. 9:666272.
doi: 10.3389/feart.2021.666272

Diana Núñez^{1*†}, Jorge A. Acosta-Hernández^{1†}, Felipe de Jesús Escalona-Alcázar^{1,2†},
Simone Pilia^{3†}, Francisco Javier Núñez-Cornú^{1†} and Diego Córdoba^{4†}

¹Sismología y Volcanología de Occidente, CUCosta, Universidad de Guadalajara, Puerto Vallarta, Mexico, ²Unidad Académica de Ciencias de la Tierra, Universidad Autónoma de Zacatecas, Zacatecas, Mexico, ³Department of Earth Sciences-Bullard Labs, University of Cambridge, Cambridge, United Kingdom, ⁴Departamento de Física de la Tierra y Astrofísica, Universidad Complutense de Madrid, Madrid, Spain

The crustal structure around the Islas Marías Archipelago has been debated for a long time. An important unresolved question is where the Rivera-North American plate subduction ends and the Tamayo fracture zone begins, from SE to NW. Results from the TsuJal project have shed light on the northwesternmost part of the Jalisco block structure. It is now clear that Sierra de Cleofas and the Islas Marías Escarpment comprise the northwestern continuation of the Middle America trench. However, other questions remain. In this paper, we present the structure of the shallow and deep crust and the upper mantle of the Islas Marías western region through the integration of multichannel seismic reflection, wide-angle seismic bathymetric and seismicity data, including records of an amphibious seismic network, OBS, and portable seismic stations, purposely deployed for this project, providing an onshore-offshore transect of 310 km length. Our findings disclose new evidence of the complex structure of the Rivera plate that dips 8°–9° underneath the NW Jalisco block as revealed by two seismic profiles parallel to the Islas Marías Escarpment. Moreover, we find five sedimentary basins and active normal faults at the edges of tectonic structures of the E-W oriented West Ranges and the N-S trending Sierra de Cleofas. Furthermore, the Sierra de Cleofas is the beginning of the active subduction of the Rivera plate beneath North America. The oceanic crust thickens and submerges towards the south while is coupled with the continental crust, from 6 km at the northern ends of the seismic profiles to 15 km in the contact region and 24 km at the coast and southern ends of them. The continental Moho was not fully characterized because of the geometry of the seismic transects, but a low-velocity layer associated with Rivera Plate subduction was observed beneath the Jalisco Block. Our results constrain the complexity of the area and reveal new structural features from the oceanic to continental crust and will be pivotal to assess geohazards in this area.

Keywords: Islas Marías archipelago, crustal structure, basins, OBS, amphibious seismic network

INTRODUCTION

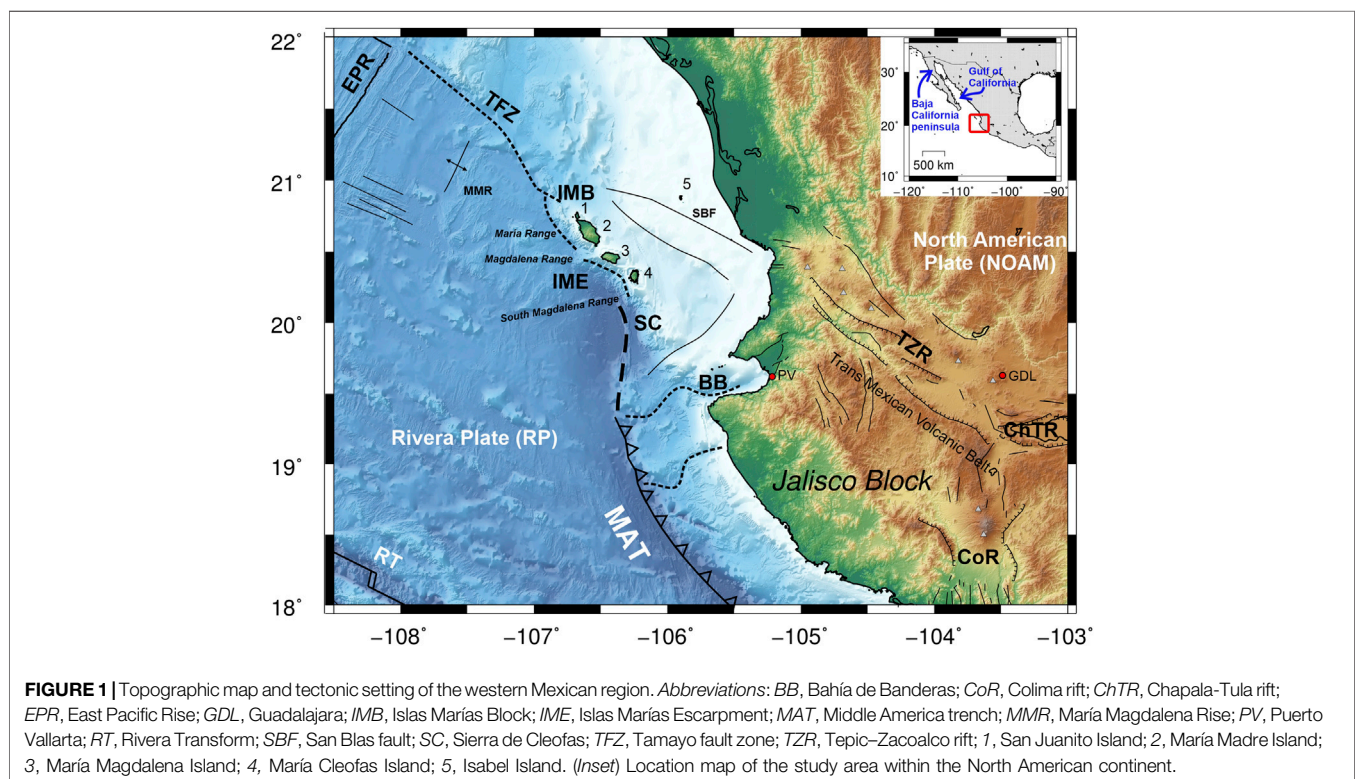
The study of active oceanic margins is the subject of numerous investigations globally, especially in regions whose boundaries are not well defined. Such is the case for the northern limit of the Rivera plate (RP). Traditionally, the northern limit has been defined as the Tamayo Fracture Zone (TFZ); however, the extent of this fracture zone and precisely where the North American plate (NOAM) begins along the region between Islas Marias and Bahía de Banderas (**Figure 1**) is not obvious. The Islas Marias Archipelago is located in the northern part of the RP and south of the Gulf of California mouth and includes San Juanito, María Madre, Magdalena, and Cleofas Islands (**Figure 1**). The origin of the islands is related to the opening of the Gulf of California (Lonsdale, 1989). This archipelago has a poorly-understood, complex tectonic history, with fragments of continental crust in several island's (San Juanito, María Madre and María Cleofas) (Pompa-Mera et al., 2013; Schaaf et al., 2015a), fragments of oceanic crust in María Magdalena (Schaaf et al., 2015b) and intraplate alkali basalts with mantle xenoliths (Isabel Island) (Ortega-Gutiérrez and González-González, 1980; Housh et al., 2010) (**Figure 1**).

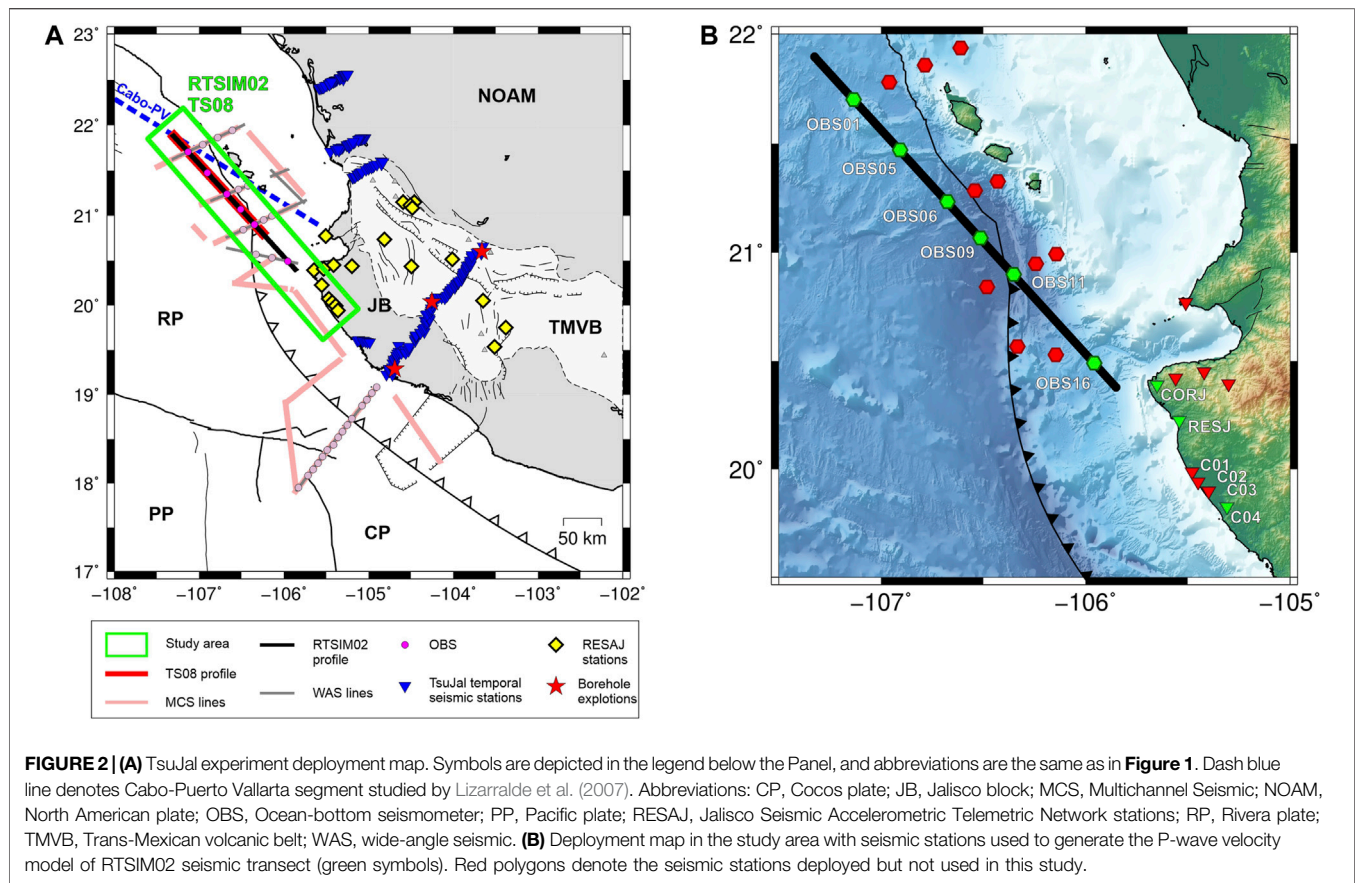
The oceanic RP originated as a fragment of the Farallon plate with independent movement starting about 10 Ma (Atwater, 1970; Lonsdale, 1989). The RP, together with the Cocos plate (CP), interact with the NOAM through active subduction, whose morphotectonic expression is the Middle America Trench (MAT). Currently, the RP subducts beneath NOAM from the northern tip of the MAT to the south and forms new seafloor along its western boundary, the Pacific-Rivera rise (DeMets and

Traylen, 2000). The southern boundary of the RP is shared with the CP and is currently defined by the transform Rivera Fault zone. Recent seismic studies of the southern boundary demonstrate that this limit is characterized by significant tectonic complexity (Núñez-Cornú et al., Submitted).

The tectonic complexity of the Islas Marias Archipelago is also evidenced by high seismicity that has generated earthquakes of moderate to large magnitudes, such as the $M > 7.0$, December 3, 1948 earthquake that occurred next to the Islas Marias Archipelago and caused significant damage to María Madre Island. Recent seismicity has been analyzed by Tinoco-Villa (2015) and constrained with the systematic recording by the Jalisco Seismic and Accelerometric Network (RESAJ in Spanish) (Núñez-Cornú et al., 2018). The historical seismicity of this region suggests that earthquakes of $M > 7.5$ have occurred. Some of the largest events occurred on June 3 and 18, 1932, with M_s 8.2 and 7.8, respectively, with an area of rupture from Bahía de Banderas to the Colima rift. In October 1995, a M_s 8.0 earthquake took place in the region, breaking only the southern half of the 1932 earthquake rupture area (Escobedo et al., 1998).

Recently, in the western Mexican margin, new geologic and marine geophysical research has been carried out to study the interaction between RP, CP, and NOAM (Núñez-Cornú et al., 2016; Dañobeitia et al., 2016; Núñez et al., 2019; Carrillo-de la Cruz et al., 2019, among others) and characterize the potentially tsunamigenic and seismogenic structures to assess geohazards and risks of this region. During the active acquisition stage of the Tsujal project, a combined off- and onshore experiment included two combined seismic methods, multichannel and wide-angle seismic, and multibeam bathymetry from Islas Marias (Nayarit





state) to the south of Manzanillo (Colima state) (**Figure 2A**) (Dañoibeitia et al., 2016; Núñez-Cornú et al., 2016). In this composite tectonic scenario, we focused on the crustal study of the western Islas Marías Archipelago. Here, we present the results by comparing a new P-wave velocity model from wide-angle seismic data with a multichannel seismic profile and hypsometric map of the northwestern boundary of the archipelago, which allow us to define the tectonic structures and interaction between RP and NOAM.

REGIONAL TECTONIC SETTING

The interactions between RP-CP and RP-NOAM characterize the active western margin of Mexico (**Figure 1**). The tectonic processes include seafloor spreading, active subduction, transform faulting, and extensional zones (DeMets et al., 1994). Within the NOAM, the inland region is characterized by two relevant geologic and tectonic features, the Trans-Mexican Volcanic Belt (TMVB) and the Jalisco block (JB). The TMVB extends from Bahía de Banderas, Nayarit, to Los Tuxtlas volcano, Veracruz, with an E-W trend and an obliqueness of 16° from its central and eastern part to the Middle American Trench (MAT) (Ferrari, 2000). This volcanic arc presents variability in the style of volcanism, geochemical affinity, and width (Gómez-Tuena et al., 2018).

The other crucial tectonic feature of the NOAM is the JB. It is considered an independent tectonic unit of the NOAM, whose separation began in the Early Pliocene as a result of the Gulf of California rifting and subsequent extension (Luhr et al., 1985). The JB structural limit to the east is the Chapala-Tula rift with 100 km length and a width from 15 to 35 km (Luhr and Carmichael, 1990). The southeastern border of the JB is defined by the Colima rift, with a range of 190 km and a width of 20–65 km, whose seaward prolongation is the El Gordo-Manzanillo rift with an NNE-SSW trend extending from the coastline to few kilometers before the intersection with the MAT (Rutz-López and Núñez-Cornú, 2004). The northern border of the JB is the NW-SE oriented Tepic-Zacoalco rift (TZR) that is 250 km in length and has an average width of 50 km (Frey et al., 2007). The northwestern extension of the JB to the RP is considered to be the Tamayo fault zone (Bourgeois and Michaud, 1991). Nevertheless, it is still not clearly defined and could also include the San Blas Fault or the Islas Marías Escarpment (IME) west of Islas Marías Archipelago.

In the offshore region, the southern and western JB boundaries correspond to the MAT. The RP is a young and small plate (Atwater, 1970), detached from the CP at about 5–10 Ma (DeMets and Traylen, 2000). Concerning the CP, NOAM, and JB, the relative movement of the RP has been the subject of study for a long time (Wilson and DeMets, 1998). The subduction of RP beneath JB is close to perpendicular to the MAT near Colima,

with a convergence rate of 5.0 cm/year to the NE (Bandy and Hilde, 2000). At the northwestern end, the convergence rate of RP beneath JB decreases to 2.0–3.0 cm/year and becomes oblique to the NNE (Kostoglodov and Bandy, 1995). Moreover, the dip angle of the subducting plate varies along the MAT. One of the first studies suggested an angle of 20° (Eissler and McNally, 1984); while Dañobeitia et al. (1997) argued that in the southern part, it is approximately 12° decreasing to the north to 7–8°. This almost-flat subduction angle has also been suggested by recent studies in this region (Gutiérrez-Peña et al., 2015; Núñez-Cornú et al., 2016; Núñez et al., 2019).

Detailed geologic and geophysical studies of the archipelago have been carried out only in recent years (e.g., Pompa-Mera et al., 2013; Schaaf et al., 2015a; Schaaf et al., 2015b; Ruiz-Martínez et al., 2016). In addition to the tectonic complexity of the poorly understood boundary between RP and NOAM, the structural and tectonic relationships between the continental and oceanic crust are vaguely understood in this region. Some seismic and tectonic studies around the archipelago provide new information about the structural characteristics to the north (Madrigal et al., 2021), west (Santibáñez-López, 2018), and south (Carrillo-de la Cruz et al., 2019). Further, the term “Islas Marías Block” (IMB) has been proposed as a tectonic unit bounded by the West Ranges, which are three linear morphological features controlled by NE-SW and NW-SE faults (Escalona-Alcázar et al., 2019).

In addition to the earthquakes caused by the subduction process between the RP and the NOAM, there are other tectonic structures in the north of the RP capable of producing seismic events of moderate magnitudes and significant seismic hazards (Marín-Mesa et al., 2019). In this region, the seismicity is principally concentrated around Sierra de Cleofas (SC) and Magdalena south fault, while in the north and east of the archipelago, seismic events are scarce (Tinoco-Villa, 2015; Núñez-Cornú et al., 2018; Escalona-Alcázar et al., 2019; Marín-Mesa et al., 2019). This scarcity could be due to the lack of seismic stations near the IMB, making it difficult to record and locate lower magnitude events or true quiescence. On December 4, 1948, an Mw 6.4 earthquake occurred at IME close to María Madre Island; the focal mechanism is consistent with high-angle reverse faults suggesting compression caused by oblique convergence in the accretionary prism (Jaramillo and Suárez, 2011). Other events occurred during January and February 2007 and September 2010 to the north and south of IMB, respectively, with Mw > 5.0. Additionally, Tinoco-Villa (2015) reported seismic swarms along the Sierra de Cleofas that could be grouped into families. The swarms occurred from October 2012 to February 2013 and were registered by the Jalisco Seismic Accelerometric Telemetric Network (RESAJ) (Núñez-Cornú et al., 2018).

DATA AND METHODOLOGIES (MATERIALS AND METHODS)

The main tectonic structures from the western region of Islas Marías to the Jalisco coast were characterized using the seismic

lines RTSIM02 and TS08 obtained during the active part of the TsuJal project (Núñez-Cornú et al., 2016). During February and March 2014, Spanish and Mexican researchers carried out the deployment and collection of multidisciplinary data offshore and onshore in western Mexico with the participation of the British oceanographic research vessel *RRS James Cook* during the cruise JC098. In a month of fieldwork, the RRS James Cook was tasked with providing the seismic source, deploying and collecting the ocean-bottom seismometers (OBSs), as well as acquiring multichannel seismic reflection (MCS), multibeam and high-resolution bathymetry, and potential fields (magnetism and gravity) data. The wide-angle seismic (WAS) data were recorded by the RESAJ stations, an on-land temporary seismic network, and the OBSs, particularly deployed for this project.

Wide-Angle Seismic Data Acquisition and Seismic Phases

The RTSIM02 seismic transect was located west of the Islas Marías, parallel to the coastline, in a northwest-southeast orientation (Figure 2A). The shooting line had an approximate length of 230 km, where 749 shots were performed. The source design was adapted to this experiment to obtain the maximum possible energy concentrated in the lowest frequency range and the maximum possible offset distance. Table 1 shows the seismic source parameters used for this transect. These shots were recorded by seismic stations located both on the continent and on the ocean bottom.

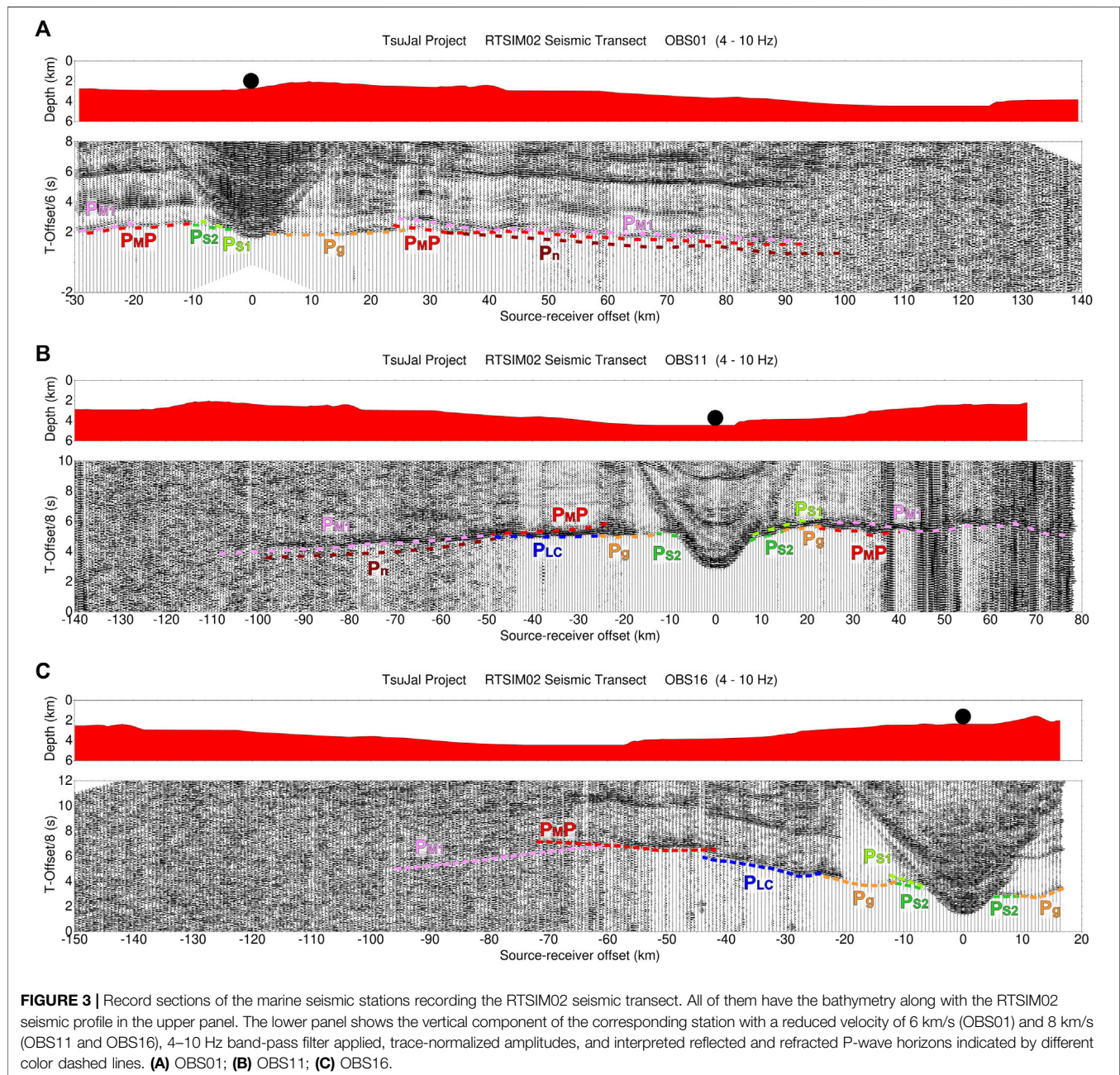
Throughout the RTSIM02 seismic profile, the WAS acquisition was recorded on six short-period OBSs (model LC2000SP with L28 three-component geophone sensors, natural frequency of 4.5 Hz), and a single HiTech HYI-90-U hydrophone deployed at OBS1, OBS5, OBS6, OBS9, OBS11, and OBS16 locations. On land, four Quanterra Q330S (Kinematics) instruments with LE-3D Lennartz sensor (1 Hz) were installed at C01, C02, C03, and C04 locations, as well as two permanent stations of the RESAJ network, were used (RESJ and CORJ) with the same type of sensors as the temporary land-based stations, making a total of 12 seismic instruments (Figure 2B). The WAS transect had a total length of 320 km.

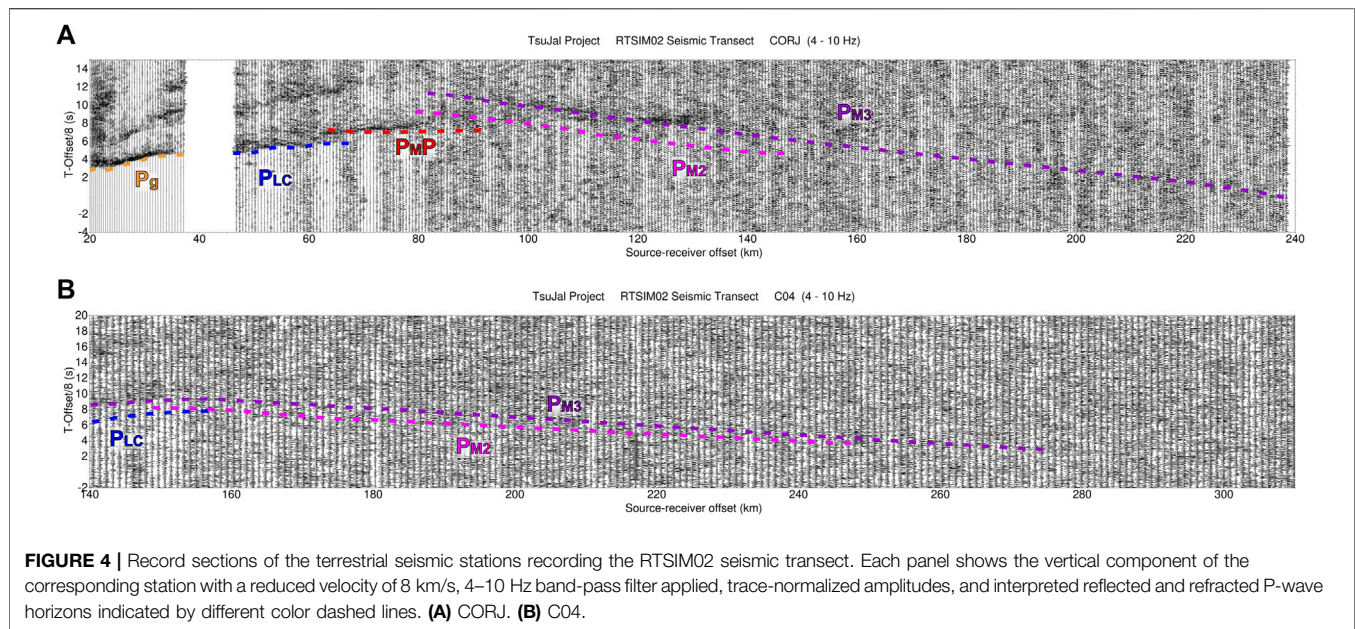
The raw seismic data were processed, including band-pass filtering and merging with navigation data, corrections due to clock drift of instruments, and zero-phase band-pass filters (4–10 Hz). Traveltime corrections follow the methodology presented in Núñez et al. (2016). The P-wave phase interpretation was completed with the bathymetry and topography data (Figures 3, 4).

P-wave refracted and reflected phases were correlated to determine the different discontinuities in the crust and the uppermost mantle along the RTSIM02 profile. The apparent velocities of refracted waves were determined for the generation of the initial velocity and depth distribution. We identified five refracted phases [two within the sediments (P_{S1} , P_{S2}), one within the crust (P_g), one in the lower crust (P_{LC}), and one within the uppermost mantle (P_n)], one reflected phase in the lower crust (P_{LCP}), one crust-mantle boundary reflection (P_{MP}),

TABLE 1 | Seismic source parameters used during the RTSIM02 wide-angle (WAS) and the TS08 multichannel seismic (MCS) data acquisition.

Seismic source parameters	WAS	MCS
Source controller	Big Shot®	Big Shot®
Source type	Bolt® G.Guns 1500LL	Bolt® G.Guns 1500LL
Air pressure	2,000 psi	2,000 psi
Volume	6,800 in ³	3,540 in ³
Compressors	4 × Hamworthy® 4 TH 565 W100	4 × Hamworthy® 4 TH 565 W100
Number of air-guns and strings	11 air-guns in 5 strings	12 air-guns in 4 strings (3 air-gun/string)
Synchronization	±0.1 ms	±0.1 ms
Deployment depth	15 m	8 m
Trigger interval	120 s	50 m





and three reflections in the first layers of the upper mantle P_{M1} , P_{M2} , and P_{M3} .

The OBS sections show phases traveling through the sediments, crust, and the most upper mantle discontinuity (Figures 3A–C), while the land station sections provide better insights into the most profound upper mantle boundaries (Figures 4A,B). A total of 5,402 first arrivals (P_{S1} , P_{S2} , P_g , P_{LC} , and P_n), P_{LCp} , P_{Mp} , and reflections in the upper mantle were manually picked. A weighted average estimation for each phase picking error was calculated (Supplementary Table S1) following the methodology proposed by Núñez et al. (2016). The picking error estimation consisted in determining the individual uncertainties in arrival time picking of every seismic phase, adding the uncertainty due to the offset distance between the seismometer position and the shooting line. This factor was significant for seismic phases recorded by land stations. The two-dimensional (2-D) velocity and structure model was obtained after assembling the travel-time interpreted picks and using the Rayinvr software (Zelt and Smith, 1992) for forward modeling, while for travel-time inversion, we applied TOMO2D (Korenaga et al., 2000). Additional water depth and elevation values from bathymetry and navigation data provided by RRS James Cook and a regional digital elevation model were included. We established the origin of the model distance along this transect from a selected point located 30 km north of the OBS01 (Figure 2).

Multichannel Seismic and Bathymetry Data

MCS data acquisition was carried out by a streamer of 5.85 km length (468 active channels, separated 12.5 m) deployed at 10 m depth. The common depth point (CDP) distance is 6.25 m, providing a CDP nominal fold of 58–59 traces. These data were sampled at 1 ms and recorded initially in SEG-D format. The technical parameters of the seismic source used in this study

are shown in Table 1. The TS08 seismic line consisted of 3,445 shots with a total length of 172 km approximately.

The MCS data processing was carried out by Seismic Unix software (Cohen and Stockwell, 2013), applying the main stages and parameters shown in Table 2. Finally, we obtain our MCS images of the TS08 seismic profile.

The bathymetric data were acquired from a Kongsberg EM120 and Kongsberg EM710 multibeam echosounders mounted aboard the RRS James Cook. Using bathythermograph (XBT) probes, sound velocity profiles in the water column were obtained daily and included during processing.

The data recovered in the area of the RTSIM02 and TS08 seismic profiles were processed using CARIS HIPS and SIPS (Teledyne) software, including sound speed and tide corrections provided by CICESE (Centro de Investigación Científica y de Educación Superior de Ensenada). During this processing stage, vertical and horizontal data produced georeferenced data, including calculating the total propagated uncertainty for each sounding. Finally, regular grid and variable resolution surfaces with different filters and editors were applied to generate the final bathymetric surface with an 80 × 80 m resolution grid, which was interpolated and depicted using System for Automated Geoscientific Analyses (SAGA) and Geographic Information Systems (GIS) (Conrad et al., 2015).

RESULTS

MCS and Bathymetry Data

The bathymetric map shows the seafloor structures and their trends (Figure 5). The structural features of the continental borderland of the JB were described by Núñez-Cornú et al. (2016), Carrillo-de la Cruz et al. (2019). However, those of the RP near the JB are poorly known. During the Tsujal project, the

TABLE 2 | Processing flow applied to the TS08 multichannel seismic profile using Seismic Unix.

Process	Parameters
Format change	SEG-D to SU
Trace and shot editing	Antialias and bad traces killed (252 and 260). Dummy events (486-495, 747-751, 811-821)
Bandpass filtering	4-6-130-150 Hz
Predictive deconvolution	Maximum lag 200 ms, minimum lag 13.4 ms
Geometry specifications	CDP gathering
Bandpass filtering	4-6-120-130 Hz
Velocity analysis	Semblance spectra, each 100 CDP
NMO correction	Velocity model
Stack	Velocity model
Second predictive deconvolution	Maximum lag 133 ms, minimum lag 5 ms
Migration	Phase-shift method

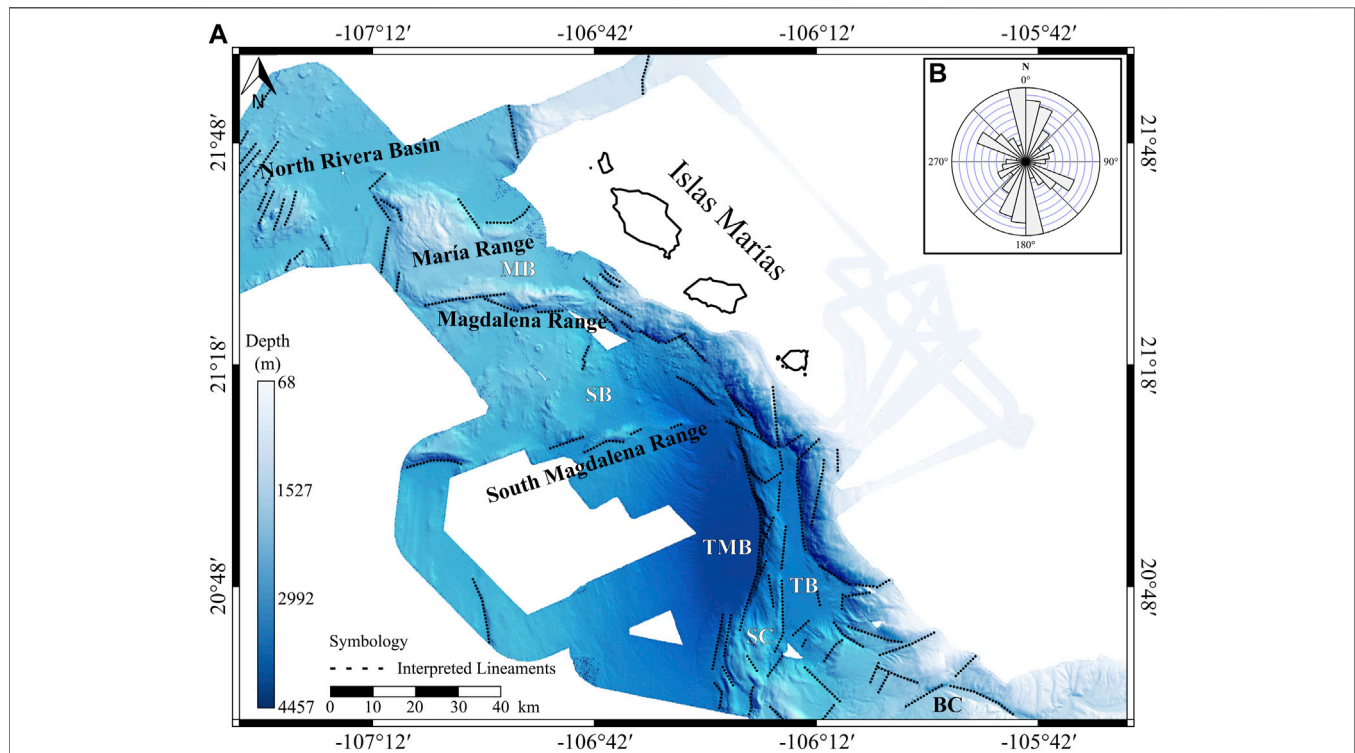
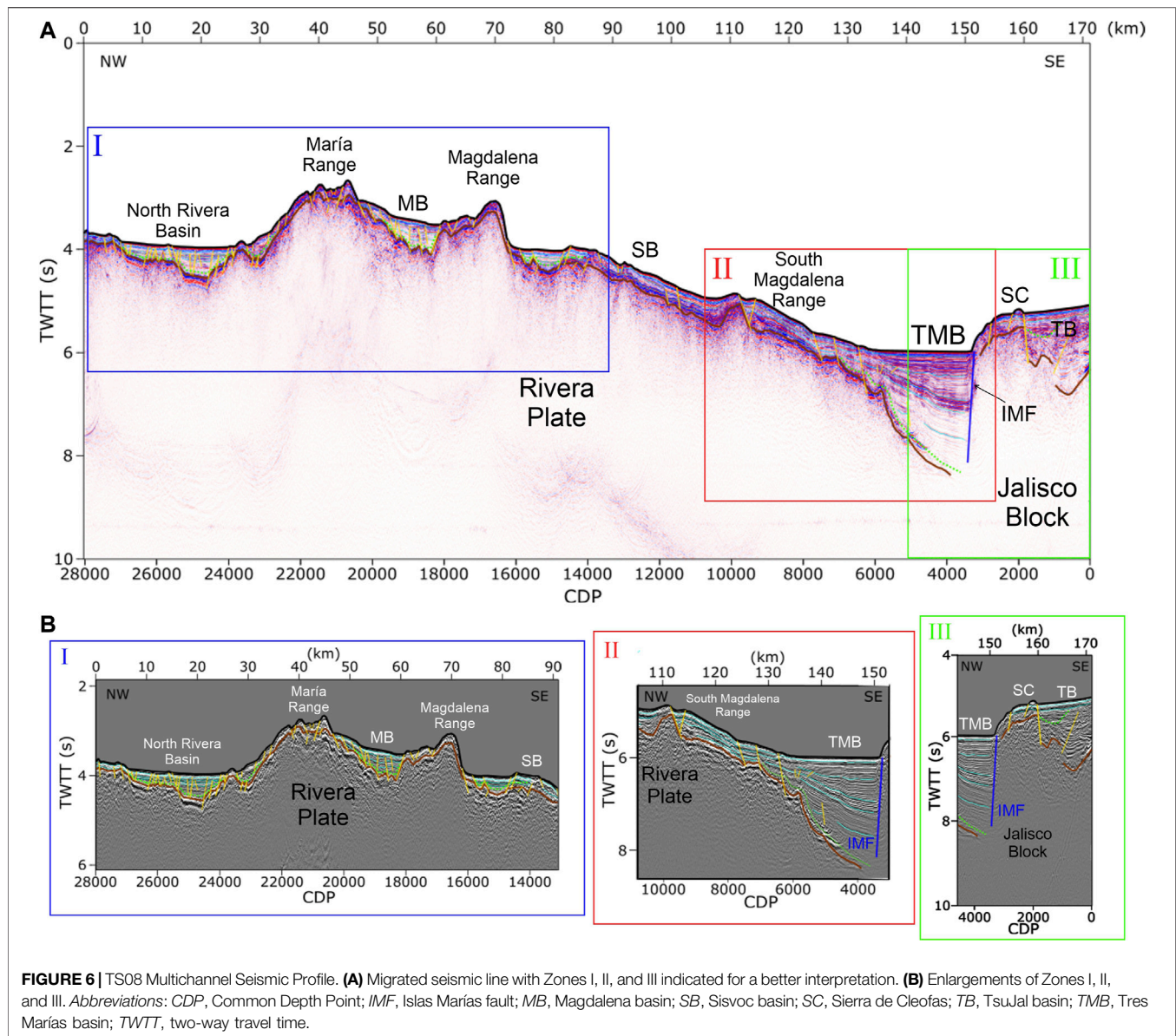


FIGURE 5 | Bathymetry map of the western Islas Marías region. **(A)** Hypsometric map with interpreted surface lineaments. **(B)** Bidirectional rose diagram of the structural features interpreted from bathymetry showing a N-S preferential tendency. Black dotted lines represent the interpreted lineaments observed. Data obtained with EM120 multibeam echosounder and processed with CARIS Hips and Sips (v.10.4). *Abbreviations:* BC, Banderas Canyon; MB, Magdalena basin; SB, Sisvoc basin; SC, Sierra de Cleofas; TB, Tsujal basin; TMB, Tres Marías basin.

new detailed bathymetry allowed us to generate a detailed seafloor map and combine it with the seismic reflectors. The seafloor patterns show that ranges and basins are structurally controlled. From NW to SE (**Figure 5A**), the Magdalena basin lies between the E-W oriented María and Magdalena ranges (Escalona-Alcázar et al., submitted). To the SE, the Sisvoc basin is limited by the ENE-WSW South Magdalena range (Escalona-Alcázar et al., submitted). To the south, this range is the northern limit of the larger Tres Marías basin (Núñez-Cornú et al., 2016) (**Figure 5A**). The continental borderland structures south of the Islas Marías Archipelago are mostly oriented N-S (**Figure 5B**)

(Carrillo-de la Cruz et al., 2019). This structural trend changes to NW-SE along the IME, being oblique to the María, Magdalena, and South Magdalena ranges.

The TS08 seismic profile is oriented NW-SE, parallel to the Islas Marías Archipelago trend and the RP. This profile was made to characterize the shallow structure west of the archipelago. We divided the seismic section into three zones (I to III) according to the structures observed (**Figure 6**). Zone I is 90 km long, counting the CDPs 28,000 to 13,500. Normal faults define the morphology; the horsts are the María and Magdalena ranges (**Figure 6B**), while the grabens are the North Rivera, Magdalena, and Sisvoc basins.



The North Rivera basin has a buried horst in the middle; the two small basins show slightly tilted seismic reflectors to the SE, with a slim splayed array. The faults are no longer active since the uppermost reflector is subhorizontal in the whole basin. The maximum sedimentary depth is 0.6 s of TWTT. The structure of the Magdalena basin are normal faults, actually inactive, showing a synthetic array. The seismic reflectors are somewhat tilted to the SE. The Magdalena and South Magdalena ranges are the Sisvoc basin, showing subhorizontal seismic reflectors in its first 10 km. Advancing to the SE, zone II (**Figure 6B**) corresponds to the southern part of the Sisvoc Basin, the South Magdalena range, and the Tres Marías basin (TMB). The acoustic basement is faulted and composed of gabbroic intrusions and basalts overlaid by thin sedimentary layers of silt and clay according to the lithologies found at the DSDP site 473 (Yeats et al., 1981). The TMB has the maximum sedimentary thickness of the profile,

equal to 2.5 s of TWTT. The main feature of this zone is the tilting to the SE and the splay array of the seismic reflectors towards the Islas Marías fault (IMF) (**Figure 6**). This array suggests that the IMF is currently active. Zone III is located in the southern part of the profile, with the IMF, SC, and TB as the main tectonic structures in this region (**Figure 6B**). The TB has 1.0 s of TWTT of sedimentary thickness, with its reflectors gently tilted to the NW.

WAS Data

Modeling of the RTSIM02 data produced a P-wave velocity model that constrains sedimentary, crustal, and uppermost mantle structures of the western region of Islas Marías to a depth of 60 km. The model origin was placed at the northwesternmost shot location of the seismic line, 29.3 km from the OBS01 (**Figure 7**).

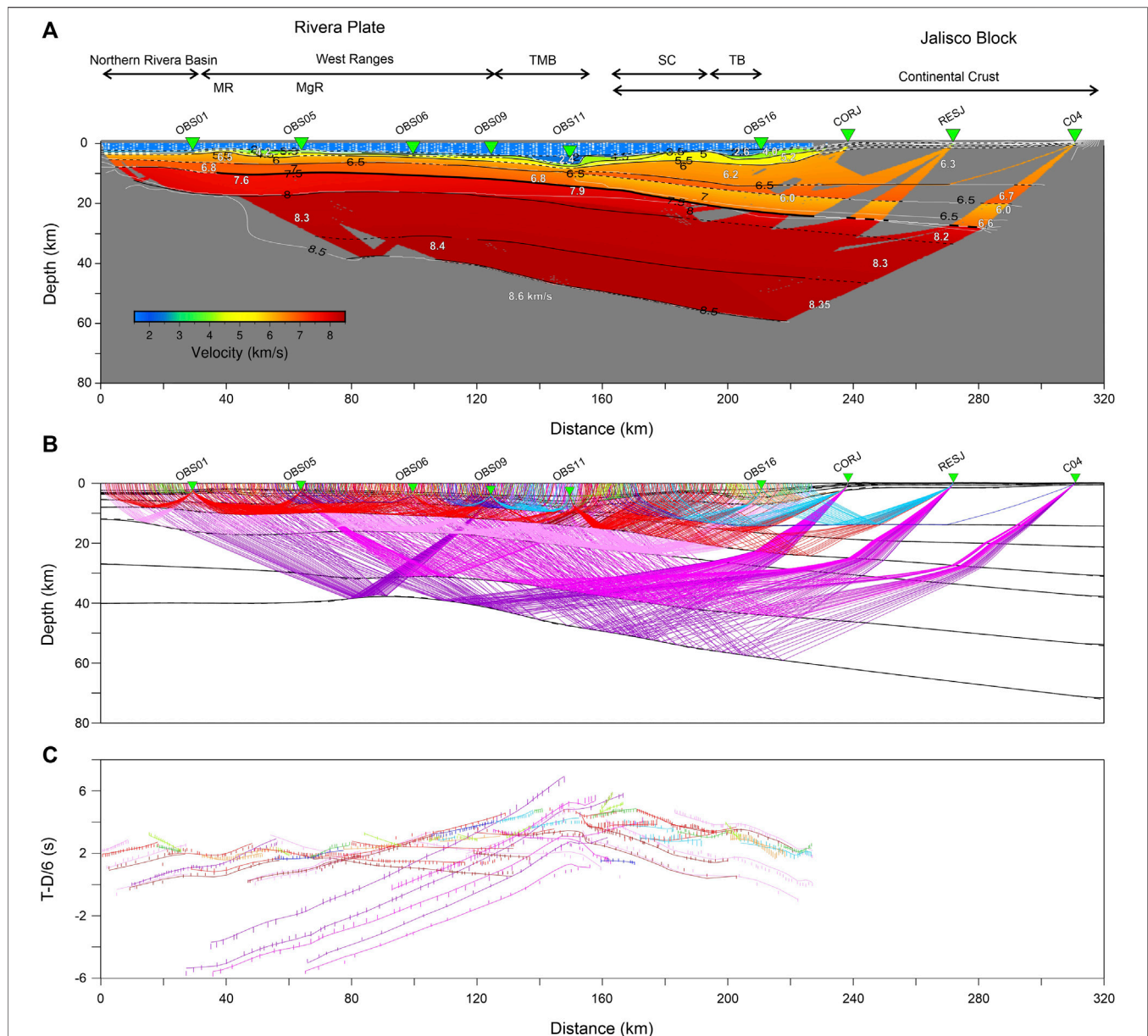
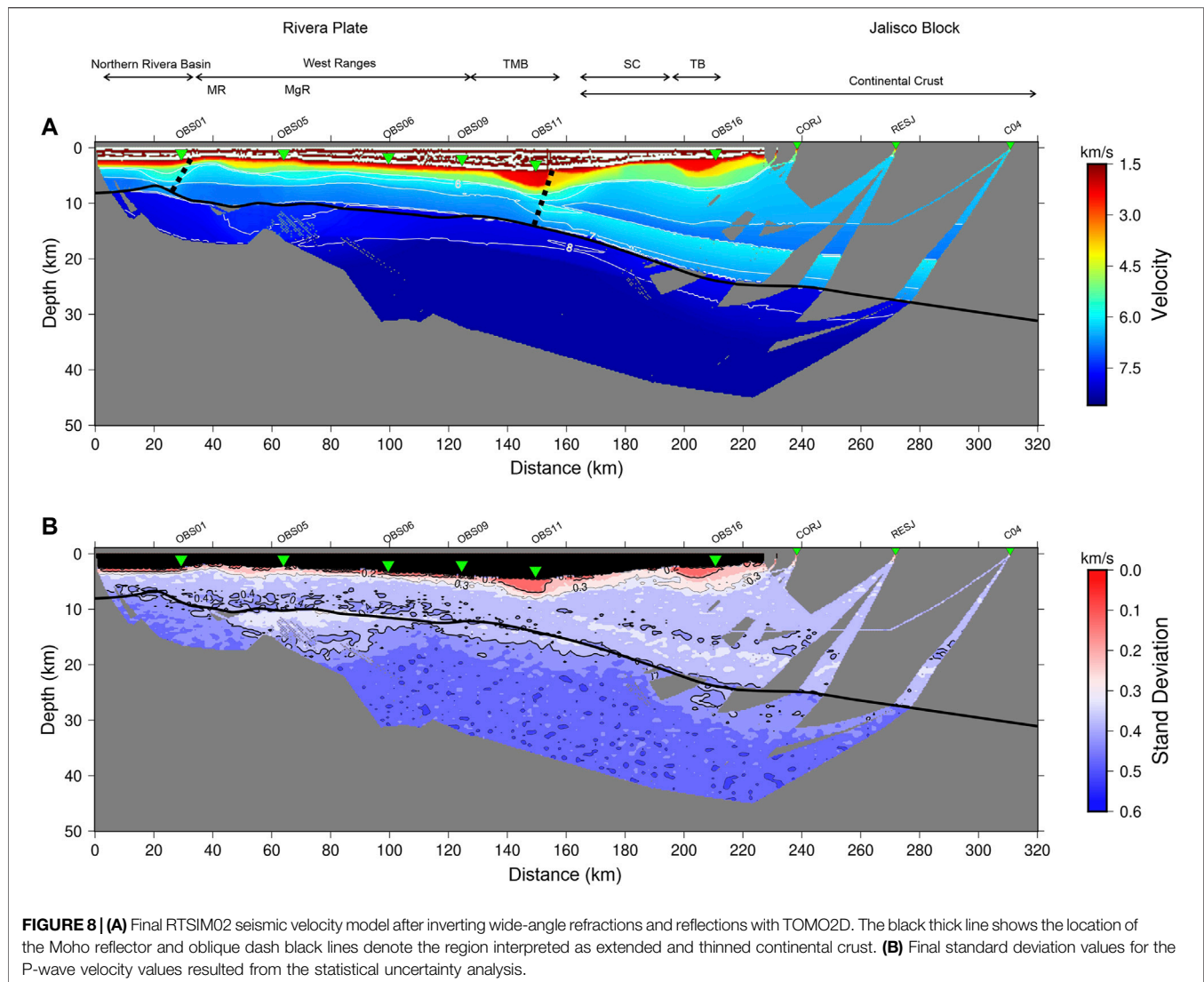


FIGURE 7 | (A) Final RTSIM02 P-wave velocity model across the western region of Islas Marías (Mexico). Black inverted triangles depict land stations of the Tsujal RTSIM02 seismic profile. Vertical and horizontal axes show depth below sea level and model position, respectively. The colored area is the region where ray tracing provides the velocity values. Black lines describe layer boundaries, and the thick ones mark positions where rays are reflected, showing the well-defined areas. The gray zone represents the area not crossed by rays. **(B)** Ray tracing and velocity model with average velocities in km/s. **(C)** Comparison between observed (vertical bars) and calculated (lines) travel times. In all panels, distances refer to the velocity model origin. *Abbreviations:* MgR, Magdalena range; MR, María range; SC, Sierra de Cleofas; TB, Tsujal basin; TMB, Tres Marias basin.

A 2 km-thick sedimentary sequence was imaged along the North Rivera Basin, composed of two layers whose velocity range varies from 2.5 km/s to 4.5 km/s top to bottom (**Figure 7A**). In the Magdalena basin, between the María and Magdalena ranges (40–50 km model distance), the sedimentary cover thickens from 2.0 to 4.6 km depth with similar velocities as the North Rivera Basin. From the Magdalena range, the Sisvoc basin throughout TMB, the seafloor deepens to ~2.0 and 4.1 km while the sediment layers are thickened 1.5–2.6 km. The TMB is characterized by a

lateral velocity variation between 2.3 and 2.4 km/s at the top and 4.1–4.3 km/s at the bottom, being the first sedimentary layer ~3 km thick. To the southeast, the Sierra de Cleofas divides the TMB from TB. The TB presents two layers of sediments with P-wave velocities of 2.4–2.6 km/s and 4.0–4.2 km/s, and thicknesses of 2.1 and 1.2 km, respectively.

In the Rivera Plate region, a thin layer is located under the sedimentary cover with P-wave velocities between 5.1 and 5.3 km/s, and its lower limit would be associated with the



acoustic basement observed in the TS08 profile. This layer has a maximum thickness of 0.5 km in the north Rivera basin region, approximately 1 km below the West Ranges (conjointly called the María, Magdalena, and South Magdalena ranges), increasing towards the TMB. In the Sierra de Cleofas and TB region up to the coastal zone, this layer appears thickened with values of 2–2.5 km, while in the continental region, the thickness decreases to values to less than 1 km.

The lower crust is characterized as thin in the oceanic region, showing a vertical gradient from 6.0–6.9 km/s with average thicknesses of 6 km and a cortical thickness between 7 and 9 km with a velocity contrast of 6.9–7.8 km/s. In the contact zone between RP and JB, the lower crust dips with an angle of 8°–9°, where the Moho is located deeper than 15 km, increasing in depth towards the coastal zone where it reaches 24 km. Due to the spatial arrangement of land seismic stations in the profile, it has not been possible to characterize continental Moho, but a low-velocity layer associated with RP subduction was observed under JB. Throughout the RTSIM02 seismic profile, we identified three

seismic layers in the upper mantle with velocities increasing in depth, reaching maximum values of 8.6 km/s at 60 km depth.

Once adjusted for travel time and controlled by amplitudes through synthetic seismogram calculations, our model reproduces 5,246 of 5,402 (97%) of observed travel times throughout the entire length of the profile (320 km). We determined the arrival-time fit quality (χ_N^2) for each interpreted phase with the following values for P_{S1} (0.8), P_{S2} (0.9), P_g (1.0), P_{LCP} (1.2), P_{LC} (1.0), P_{MP} (1.0), P_r (0.9), and reflected P-phases observed in the mantle P_{M1} (1.6), P_{M2} (1.3), and P_{M3} (1.2). Our final model is not far from the ideal case ($\chi_N^2 = 1$) producing a χ_N^2 of 1.2 (**Supplementary Table S1**).

Tomography and Resolution

The seismic structure of the western Islas Marías Archipelago along RTSIM02 is constrained by the inversion of our wide-angle seismic travel time data for the previous 2D P-wave velocity model. We used a layer stripping strategy to find a seismic velocity model that fits our data by linear inversions. First, we

carried out an inversion of 897 first-arriving crustal phases (P_{S1} , P_{S2} , P_g , and P_{LC}) to create a smooth image of the seismic velocity structure with a root-mean-square misfit of 0.17 s. Secondly, we incorporated the P_{MP} phases (1,087 travel-time picks) in our inversion with the initial Moho discontinuity reflector obtained from the previous forward 2D seismic velocity model. For the last inversion, P_n phases (978 travel-time picks) and Moho reflector obtained from the previous inversion were included. Our simultaneous wide-angle refraction and reflection travel-times inversion constrains the boundary depths and velocities of the crust and upper mantle throughout our seismic profile (**Figure 8A**). We used a total of 2,962 travel-time picks.

The uncertainty of our velocity model was determined by calculating the standard deviation of successful inversions of 100 Monte Carlo realizations is shown in **Figure 8B**. From seafloor to basement, the standard deviation obtained is less than 0.3 km/s, which increases until 0.4 km/s close to Moho depth. Below Moho, maximum values of standard deviation are less than 0.6 km/s.

The P wave velocity distribution and their standard deviation shown in **Figure 8** clearly define the Moho. Its depth varies between 9–11 km until the OBS11, increasing up to 25 km at the OBS16 in the Tres Mariás Fault.

DISCUSSION

Other studies in Western Mexico have used a variety of seismic techniques to understand the tectonic relationship between the various tectonic plates and formation of their related structures (Dañoibeitia et al., 1997; Fabriol et al., 1999; Aragón-Arreola et al., 2005; Lizarralde et al., 2007; Brothers et al., 2012; Núñez-Cornú et al., 2016; Núñez et al., 2019; Carrillo-de la Cruz et al., 2019; among others). The region of the Gulf of California and the tectonic processes involved have been addressed with different seismic techniques. The crustal structure at the mouth of the gulf region was defined by wide-angle seismic profiles that included OBS and land stations (Lizarralde et al., 2007).

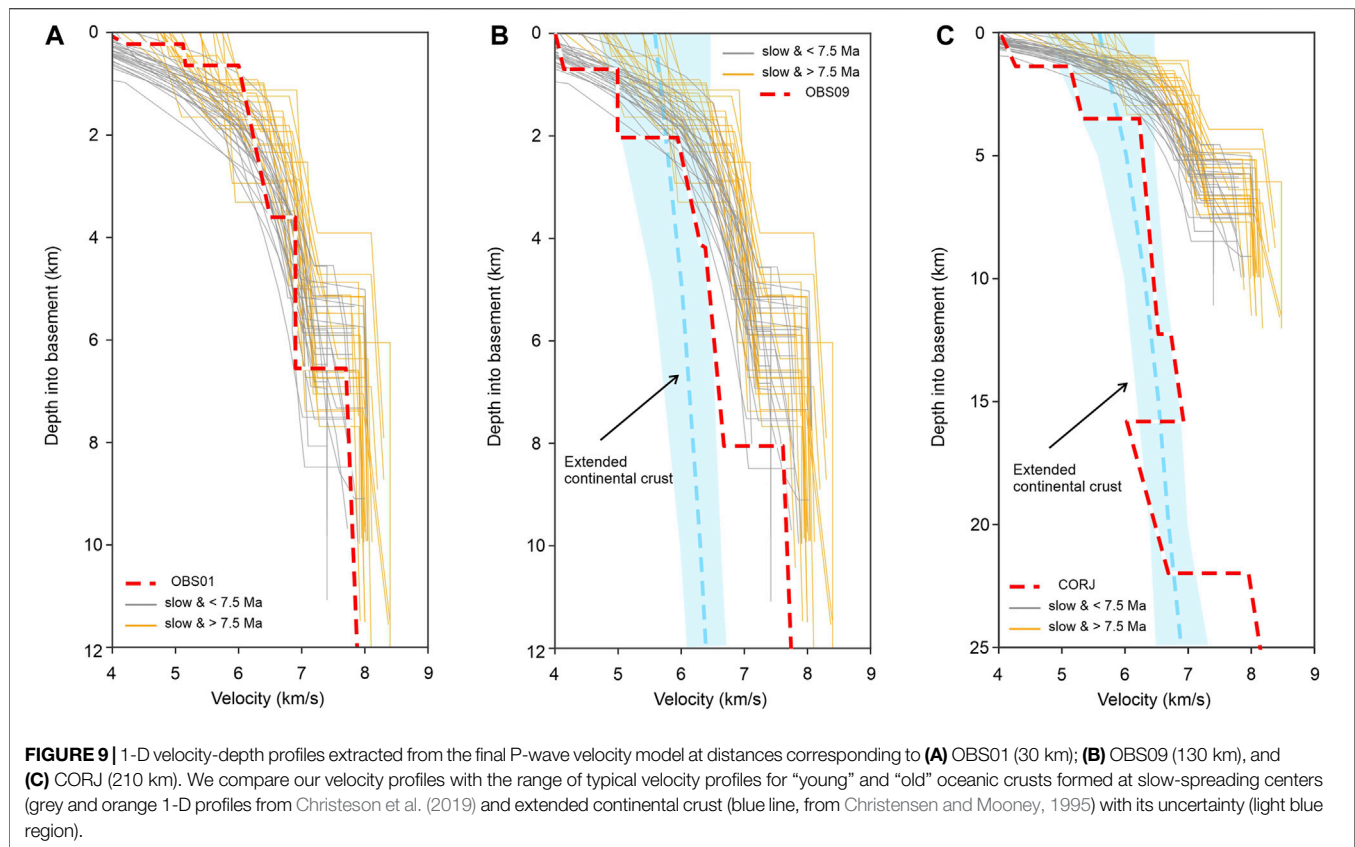
Some experiments used multichannel and wide-angle seismic profiles, either with or without OBS and land stations, perpendicular to the main structural trend of the Gulf of California (e.g., Fabriol et al., 1999; Aragón-Arreola et al., 2005; Brothers et al., 2012; Macías-Iñiguez et al., 2019), finding that the end of the continental crust is a sharp zone along most of the eastern margin of Baja California. However, in the eastern margin of the gulf, there is an ocean-continent transition zone with extension and thinned continental crust. These studies suggest different rifting and basin evolution styles, some of them with related volcanism and others without, based on the thermal state of the mantle and the rigidity of the lower crust (Lizarralde et al., 2007).

In the region between Puerto Vallarta and Los Cabos and extending a bit further to the NW within the gulf, the geophysical, multichannel, and wide-angle seismic profiles were carried out with general NW-SE orientation, such that the trend of these profiles is perpendicular to the ridges in the Gulf of California and

the East Pacific Rise (Lizarralde et al., 2007; Páramo et al., 2008; Sutherland et al., 2012; Abera et al., 2016). From the western Mexico coastline to the SW, the results obtained from the seismic and geophysical profiles have revealed different deformation styles and structures. Close to the western Mexican continental margin, the Tamayo Banks were defined as a microcontinent (Abera et al., 2016), bound to the SW by the Tamayo fracture zone, while to the NW is the Alarcón basin with oceanic crust. The SE limit is the Tamayo trough, an extended portion of continental crust with poor oceanic crust development (Lizarralde et al., 2007; Sutherland et al., 2012; Abera et al., 2016). Next to the SE is the San Blas basin, the largest in the region, built on continental crust, with a sedimentary thickness of 2 s of TWTT and slightly deformed (Sutherland et al., 2012).

Previous seismic profiles west of the Islas Mariás Archipelago have different lengths and different levels of detail. Páramo et al. (2008) made multichannel seismic profiles from Los Cabos to the East Pacific Rise (EPR), 150 km west of the Islas Mariás Archipelago. The horst and graben array found in the continental crust and the sharp ocean-continent transition are similar to those found along the western gulf coast. There is evidence of syndepositional deformation and post tectonic sedimentation (Páramo et al., 2008). Lizarralde et al. (2007) presented the wide-angle seismic profile from Los Cabos to Puerto Vallarta close to the RTSIM02 and TS08 profiles. From NW to SE, Lizarralde et al. (2007) showed the oceanic crust of the María Magdalena Rise, followed by a thinned continental crust with a thin sedimentary cover until it reaches the Sierra de Cleofas. The velocity model has a lower crust with velocities of 6 km/s, which were associated with granitic rocks, velocities of ~5 km/s were associated with volcanic and sedimentary rocks, and those of <3 km/s related to sediments (Lizarralde et al., 2007; Páramo et al., 2008). In our velocity model (**Figure 8A**), the thinned continental crust region is defined from the West Ranges to Tres Mariás basin and Sierra de Cleofas, with small basins in between (Magdalena and Sisvoc basins). The area along the profile TS08/RTSIM02 is in the seaside west of the IMF, oriented NW-SE. Its location offers a unique opportunity to understand the nature of the crust immediately west of the Islas Mariás Archipelago. Along our seismic profile (**Figure 8A**), around OBS05 to OBS11 (next of the IMF), we observe a thin and continuous layer of ~1 km thickness with velocities belonging to granitic and volcanic/sedimentary rocks. This cover is underlain by ~5 km thick lower crust. These crustal velocities are in agreement with those reported from 6.0 to 6.6 km/s for the average continental crust in this region (Chulick and Mooney, 2002); nonetheless, it is only ~6 km thick. Below it, the velocity increases to >7 km/s, typical values at the base of layer 3 for the oceanic crust (Christeson et al., 2019). The velocity distribution varies from ~3 to 6.6 km/s, except in the TMB, where it decreases to 2.4 km/s due to the sedimentary cover thickening. Our velocity model is similar to that from Lizarralde et al. (2007); however, ours is able to characterize the uppermost part of the crust.

We compare three 1-D velocity–depth profiles across our seismic transect with compilations made for young and old oceanic crust formed at slow-spreading centers (age <7.5 Ma,

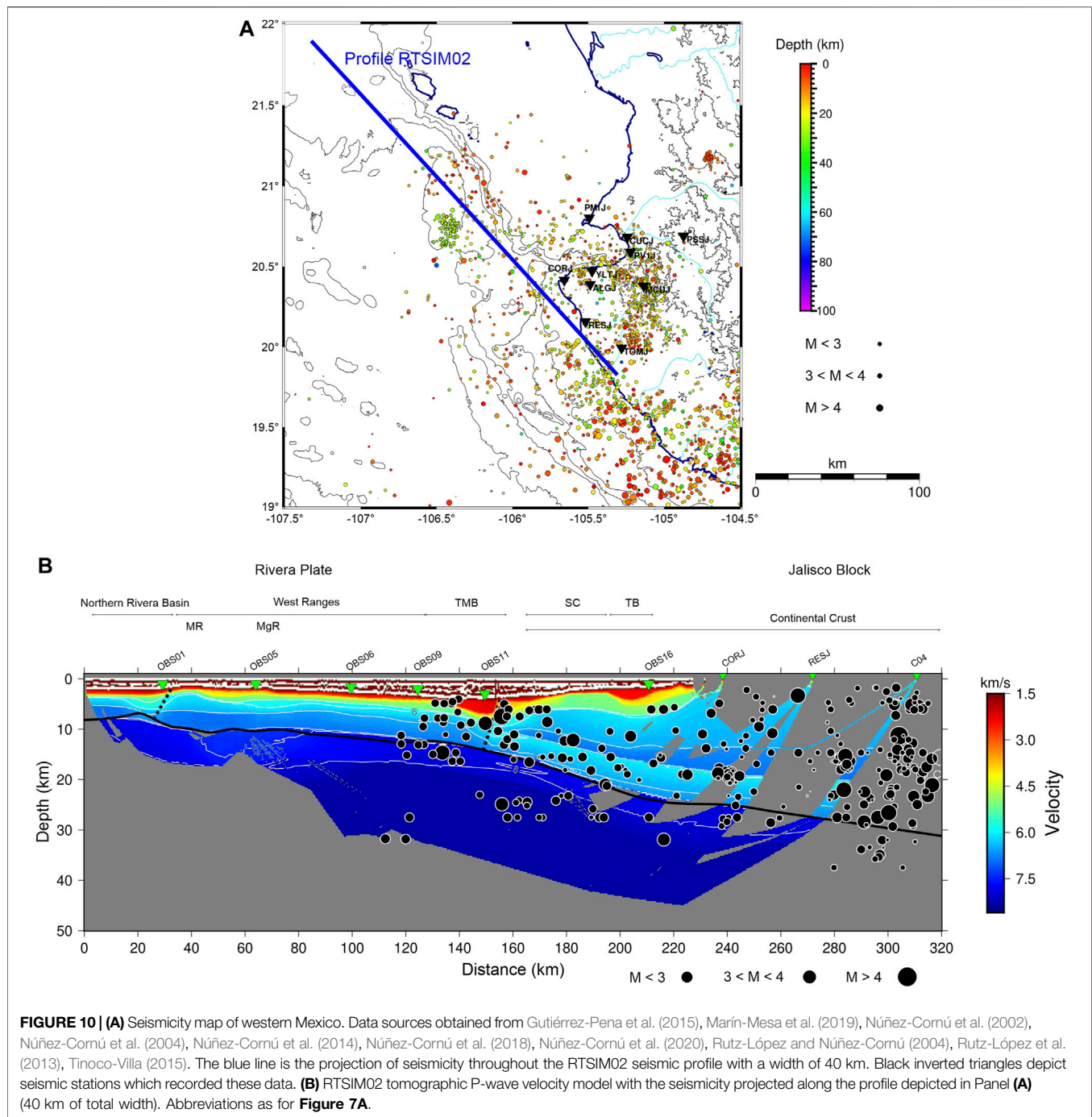


> 7.5 Ma and 5–20 mm/yr half spreading rate, respectively, as defined by Christeson et al. (2019) as in Pilia et al. (2021). **Figure 9A** shows that our profile located at 30 km (OBS01) in the North Rivera Basin suggests velocities and thicknesses close to those reported for the young oceanic crust and according to RP age which is <7.5 Ma with possible remnants that could reach ca. 9 Ma (Lonsdale, 1989). However, in **Figure 9B**, our 1D velocity–depth profile at 130 km close to OBS09 (NE boundary of the Tres Marias Basin) is slower than the models of slow-spreading ridges (Christeson et al., 2019). This difference could be associated with the transition from oceanic to an extended and thinned continental crust, as proposed in the velocity model (**Figure 8A**), and could be related to gabbroic intrusions associated with the oceanic crust lithologic assemblage of María Magdalena Island (Schaaf et al., 2015b). **Figure 9C** also shows velocities slower than the young and old oceanic crust models characteristic of continental crust that is slightly extended in this region.

Our final velocity model in **Figure 8A** depicts a subparallel velocity distribution that gently becomes deeper and dips towards the SE. The velocities and thicknesses that characterize the crust have been considered as a continent-ocean transition (COT) in places like the Labrador Peninsula (Keen et al., 2018), the Flemish cap (Funck et al., 2003), or the South China Sea (Cameselle et al., 2015). In addition, due to the more detailed data, we were able to define the dip of the lower crust and the shallow structure of the NE edge of the Rivera plate. Based on our seismic reflection

profile (**Figure 6**) and the velocity distribution (**Figure 8A**), the extended and thinned continental crust could vary from extended to extremely extended. From NW to SE the structural array is of horst (María, Magdalena and South Magdalena ranges) and grabens (Magdalena, Sisvoc and Tres Marias basins). In some parts, the extension could be large enough to break the continental crust and develop an oceanic one like the lithologic assemblage described in María Magdalena Island (Schaaf et al., 2015b). The lower crust gently dips to the SE until the Sierra de Cleofas with an angle of 8°–9° beneath the NW part of the Jalisco Block.

Our model integrated the bathymetric, multichannel, and wide-angle seismic data, together with the regional seismicity (see references in **Figure 10A**). Along with the TS08 multichannel seismic profile (**Figure 6**), the seismic reflectors are gently tilted to the SE and indicate post-depositional deformation in the North Rivera and Magdalena basins. In the northern part of the Sisvoc basin, the seismic reflectors are subhorizontal; then, they tilt to the SE until the northern fault bounding the South Magdalena range, where reflectors have a slight splay array towards this fault, suggesting that it is currently active. This observation is constrained by the seismicity around the region between the OBS9 and OBS11 (**Figure 9**). From the south of the Magdalena range, the seismic reflectors are faulted and tilted, following the slope direction. Although the sediments are faulted, these structures do not extend until the top of the sedimentary coverage; they are over-filled with thin post-rift sediments. At



the change in slope, the reflectors dip, following it. Like in the Sisvoc basin, the lower sedimentary fill is faulted in the Tres Marias basins, while the uppermost layers are not. These faults are in an antithetic array with respect to Sierra de Cleofas (Figure 6). Covering the faults, the sedimentary layer is thin in the slope, but it thickens in the Tres Marias basin towards the SC, reaching a maximum sedimentary thickness of 1.7 s of TWTT with a splay array towards the fault (Figure 6).

Figure 10A shows the compilation of seismicity data in the study region carried out by the research group CA- SisVOC from

different studies between 2002 and 2016 (Gutiérrez-Pena et al., 2015; Marín-Mesa et al., 2019; Núñez-Cornú et al., 2002; Núñez-Cornú et al., 2004; Núñez-Cornú et al., 2014; Núñez-Cornú et al., 2018; Núñez-Cornú et al., 2020; Rutz-López and Núñez-Cornú, 2004; Rutz-López et al., 2013; Tinoco-Villa, 2015). These data belong to different projects that SisVOC has been involved with, including RESAJ, MARS, and individual research projects. The hypocenters depicted were located using at least four P-phase and four S-phase readings. In some cases, P-Pn times were used to constrain hypocentral depths (Urías-Espinosa et al., 2016). The

criteria applied to select the better location were: root-mean-square (RMS) arrival time error <0.5 s, the epicentral and focal depth standard errors (ERH and ERZ, respectively) < 10.0 km. In the RP-JB contact region, the seismicity is mainly located above 40 km depth, which increases landward where the hypocenters reach maximum depths of 60 km at the coast. The hypocenter distribution shown in **Figure 10A** is in the uppermost part of the lithospheric mantle, the COT and the continental crust. These events are from the TMB towards the continent, being more abundant at the continental crust. The events distribution from TMB to TB could be related to the unbalanced stress and accommodation due to the NE movement of the Rivera Plate against the NW movement of the Jalisco Block. Both structural blocks could be coupled moving together, producing seismicity along the major faults. Previous studies in this region establish focal mechanisms of high-angle reverse faulting obtained from seismograms collected from regional and teleseismic stations (Jaramillo and Suárez, 2011), which could also be associated with the oblique convergence between RP and NAP. Additionally, the NW orientation of the MAT, whose end is bending towards the north, starts the N-S oriented Sierra de Cleofas (**Figure 1**), contributing to the unbalanced forces and the seismicity. Moreover, the splay array of the sedimentary reflectors in the TMB towards the IMF at the western edge of the Sierra de Cleofas suggests that the IMF is an active fault (**Figure 6B**).

Figure 10B shows the seismicity projected in a line of 320 km coincident with our RTSIM02 tomography velocity model (**Figure 8A**) with a total width of 40 km (20 km wide on each side of the line) to compare to the WAS and MCS results. The correlation between both data sets shows consistency with the structures we propose. Moreover, we observe that the seismicity data indicate the slab is subducting in this zone with a dip angle of 8° approximately, as previously was reported by Carrillo-de la Cruz et al. (2019) and less than reported by Núñez-Cornú et al. (2016).

The faults bounding the Sierra de Cleofas are active since the seismicity is widespread around it (**Figure 10**). Further research using the RESAJ network, as well as the records from the seismic stations installed in María Madre and María Cleofas islands, could improve the locations, depth, and azimuth coverage of the seismicity presents in the Islas Marias to determine the focal mechanisms and improve the tectonic evolution knowledge of the NW boundary of the Jalisco Block and its interaction with the Rivera Plate.

CONCLUSION

The new multidisciplinary data acquired in the west of the Islas Marias Archipelago have allowed us to establish the cortical architecture of the transition between the oceanic crust of the Rivera Plate and the extended and thinned continental crust, where, from NW to SE, it is formed by the North Rivera basin, María range, Magdalena basin, Magdalena range, Sisvoc basin, South Magdalena range, and the Tres Marias basin. These new ranges and basins are defined along the RTSIM02 and TS08 profiles obtained

by the new bathymetric and OBS–land stations combined wide-angle and multichannel seismic data.

The basins to the north of the South Magdalena range contain sedimentary cover that records the faulted syn-rift deposits covered by a thin post-rift sedimentary layer. The faults along the profile are active and inactive. Inactive faults cross-cut the lowermost sedimentary layers of the basins along with the profile. Simultaneously, active faults are located at the northern limit of the South Magdalena range and the Sierra de Cleofas, evidenced by the seismicity and the splay array of the sedimentary strata, where we establish the beginning of the northernmost active subduction between the Rivera and North American plates. In this region, the bottom of the crust dips from 8° to 9° .

This study contributes to the knowledge of the active tectonic structures in the Islas Marias Archipelago region, with potential implications on geohazard identification and associated risks in this area.

DATA AVAILABILITY STATEMENT

The original contributions presented in the study are included in the article/**Supplementary Materials**, further inquiries can be directed to the corresponding author.

AUTHOR CONTRIBUTIONS

DN: Conceptualization, methodology, investigation, data processing, data analysis, conclusions, and original draft writing. JA-H: Data processing, investigation. FE-A: Data analysis, methodology, investigation, original draft writing, and conclusions. SP: Data analysis, methodology, review and conclusions. FN-C: Conceptualization, funding acquisition, methodology, investigation, review, and editing. DC: Funding acquisition, review, and editing.

FUNDING

This research was mainly funded by Consejo Nacional de Ciencia y Tecnología (CONACYT) –FOMIXJal (2012-08-189963) (Mexico), CGL (2011-29474-C02-01) (TsuJal Project) and RTI 2018-094827-B-C21 (KUK AHPAN Project) DGI Plan Nacional I + D + i (Spain); RESAJ network was funded by CONACYT–FOMIXJAL 2008–96538 (2009) (Mexico). JA-H was financially supported by a master fellowship from CONACYT with code 401435 and CVU 660422.

ACKNOWLEDGMENTS

The authors gratefully acknowledge Wendy McCausland for her valuable comments and observations, including the English grammar revision that help to improve this article and Juan Luis Carrillo-de la Cruz for his help with bathymetric and 1-D velocity-depth profiles figures. The authors also truly appreciate

the collaboration during the Tsujal project of NOC Cruise JC098, RRS James Cook (United Kingdom); COIP/COPO/UNAM J-GAP2013 Cruise (BO El Puma); Unidad de Tecnología Marina (Spain); Secretaría de Marina (Mexico) ARM Holzinger; Secretaría de Defensa Nacional (Mexico); Unidad Municipal de Protección Civil y Bomberos (Jalisco State, Mexico); Unidad Municipal de Protección Civil y Bomberos (Puerto Vallarta, Mexico); Unidad Estatal de Protección Civil y Bomberos (Nayarit State, Mexico); Reserva de la Biosfera (Islas Marías) CONANP-SEMARNAT; Secretaría de Relaciones Exteriores (Mexico); and Órgano Desconcentrado de Prevención y Readaptación Social de la SEGOP. Some figures

were generated using the Generic Mapping Tools (GMT-6; Wessel et al., 2019). SP acknowledges support from the European Union's Horizon 2020 research and innovation programme under Marie Skłodowska-Curie Grant Agreement 790203.

SUPPLEMENTARY MATERIAL

The Supplementary Material for this article can be found online at: <https://www.frontiersin.org/articles/10.3389/feart.2021.666272/full#supplementary-material>

REFERENCES

- Abera, R., van Wijk, J., and Axen, G. (2016). Formation of continental Fragments: The Tamayo Bank, Gulf of California, Mexico. *Geology* 44, 595–598. doi:10.1130/G38123.1
- Aragón-Arreola, M., Morandi, M., Martín-Barajas, A., Delgado-Argote, L., and González-Fernández, A. (2005). Structure of the Rift Basins in the central Gulf of California: Kinematic Implications for Oblique Rifting. *Tectonophysics* 409, 19–38. doi:10.1016/j.tecto.2005.08.002
- Atwater, T. (1970). Implications of Plate Tectonics for the Cenozoic Tectonic Evolution of Western North America. *Geol. Soc. America Bull.* 81, 3513–3536. doi:10.1130/0016-7606(1970)81[3513:iopftf]2.0.co;2
- Bandy, W. L., and Hilde, T. W. C. (2000). “Morphology and Recent History of the ridge Propagator System Located at 18° N, 106° W,” in *Cenozoic Tectonics and Volcanism of Mexico. Geol. Soc. Am. Spec. Paper 334*. Editors H. Delgado-Granados, G. Aguirre-Díaz, and J. M. Stock (Boulder, Colorado), 29–40. doi:10.1130/0-8137-2334-5.29
- Bourgeois, J., and Michaud, F. (1991). Active Fragmentation of the North America Plate at the Mexican Triple junction Area off Manzanillo. *Geo-Marine Lett.* 11, 59–65. doi:10.1007/BF02431030
- Brothers, D., Harding, A., González-Fernández, A., Holbrook, W. S., Kent, G., Driscoll, N., et al. (2012). Farallon Slab Detachment and Deformation of the Magdalena Shelf, Southern Baja California. *Geophys. Res. Lett.* 39, a–n. doi:10.1029/2011GL050828
- Cameselle, A. L., Ranero, C. R., Franke, D., and Barckhausen, U. (2015). The Continent-Ocean Transition on the Northwestern South China Sea. *Basin Res.* 29, 73–95. doi:10.1111/bre.12137
- Carrillo-de la Cruz, J. L., Núñez, D., Escalona-Alcázar, F. J., Núñez-Cornú, F. J., González-Fernández, A., Córdoba, D., et al. (2019). Tectonic Analysis of the Southern of María Cleofas Island from Bathymetric and Seismic Data. *Seismol. Res. Lett.* 90, 1748–1755.
- Christensen, N. I., and Mooney, W. D. (1995). Seismic Velocity Structure and Composition of the continental Crust: A Global View. *J. Geophys. Res.* 100, 9761–9788. doi:10.1029/95jb00259
- Christeson, G. L., Goff, J. A., and Reece, R. S. (2019). Synthesis of Oceanic Crustal Structure from Two-Dimensional Seismic Profiles. *Rev. Geophys.* 57 (2), 504–529. doi:10.1029/2019rg000641
- Chulick, G. S., and Mooney, W. D. (2002). Seismic Structure of the Crust and Uppermost Mantle of North America and Adjacent Oceanic Basins: A Synthesis. *Bull. Seismological Soc. America* 92, 2478–2492. doi:10.1785/0120010188
- Cohen, J. K., and Stockwell, J. W., Jr. (2013). *CWP/SU: Seismic Un*x Release No. 43R4: An Open Source Software Package for Seismic Research and Processing*. Center for Wave Phenomena, Colorado School of Mines.
- Conrad, O., Bechtel, B., Bock, M., Dietrich, H., Fischer, E., Gerlitz, L., et al. (2015). System for Automated Geoscientific Analyses (SAGA) V. 2.1.4. *Geosci. Model. Dev.* 8, 1991–2007. doi:10.5194/gmd-8-1991-2015
- Dañoibeitia, J., Bartolomé, R., Prada, M., Nuñez-Cornú, F., Córdoba, D., Bandy, W. L., et al. (2016). Crustal Architecture at the Collision Zone between Rivera and North American Plates at the Jalisco Block: Tsujal project Geodynamics of the Latin American Pacific Margin. *Pure Appl. Geophys.* 173, 3553–3573. doi:10.1007/978-3-319-51529-8_18
- Dañoibeitia, J. J., Córdoba, D., Delgado-Argote, L. A., Michaud, F., Bartolomé, R., Farrán, M., et al. CORTES-P96 Working Group (1997). Expedition Gathers New Data on Crust beneath Mexican West Coast. *Eos Trans. AGU* 78, 565–572. doi:10.1029/97eo00338
- DeMets, C., Gordon, R. G., Argus, D. F., and Stein, S. (1994). Effect of Recent Revisions to the Geomagnetic Reversal Time Scale on Estimates of Current Plate Motions. *Geophys. Res. Lett.* 21, 2191–2194. doi:10.1029/94gl02118
- DeMets, C., and Traylen, S. (2000). Motion of the Rivera Plate since 10 Ma Relative to the Pacific and North American Plates and the Mantle. *Tectonophysics* 318, 119–159. doi:10.1016/s0040-1951(99)00309-1
- Eissler, H. K., and McNally, K. C. (1984). Seismicity and Tectonics of the Rivera Plate and Implications for the 1932 Jalisco, Mexico, Earthquake. *J. Geophys. Res.* 89, 4520–4530. doi:10.1029/jb089ib06p04520
- Escalona-Alcázar, J. F., Núñez-Cornú, J. F., Núñez, D., and Córdoba-Barba, D. (2019). A Bathymetric and Structural Analysis of the Islas Marías Archipelago, Mexico, and Surroundings. *Submitted J. Struct. Geology*, 90, 1748–1755. doi:10.1785/0220180398
- Escobedo, D., Pacheco, J. F., and Suárez, G. (1998). Teleseismic Body-Wave Analysis of the 9 October, 1995 (Mw = 8.0), Colima-Jalisco, Mexico Earthquake, and its Largest Foreshock and Aftershock. *Geophys. Res. Lett.* 25, 547–550. doi:10.1029/98gl00061
- Fabriol, H., Delgado-Argote, L. A., Dañoibeitia, J. J., Córdoba, D., González, A., García-Abdeslem, J., et al. (1999). Backscattering and Geophysical Features of Volcanic Ridges Offshore Santa Rosalia, Baja California Sur, Gulf of California, Mexico. *J. Volcanology Geothermal Res.* 93, 75–92. doi:10.1016/S0377-0273(99)00084-0
- Ferrari Pedraglio, L. (2000). Avances en el conocimiento de la Faja Volcánica Transmexicana durante la última década. *Bsgm* 53, 84–92. doi:10.18268/bsgm2000v53n1a5
- Frey, H. M., Lange, R. A., Hall, C. M., Delgado-Granados, H., and Carmichael, I. S. E. (2007). A Pliocene Ignimbrite Flare-Up along the Tepic-Zacoalco Rift: Evidence for the Initial Stages of Rifting between the Jalisco Block (Mexico) and North America. *Geol. Soc. America Bull.* 119, 49–64. doi:10.1130/B25950.1
- Funck, T., Hopper, J. R., Larsen, H. C., Loudon, K. E., Tucholke, B. E., and Holbrook, W. S. (2003). Crustal Structure of the Ocean-Continent Transition at Flemish Cap: Seismic Refraction Results. *J. Geophys. Res.* 108, 2531. doi:10.1029/2003JB002434
- Gómez-Tuena, A., Mori, L., and Straub, S. M. (2018). Geochemical and Petrological Insights into the Tectonic Origin of the Transmexican Volcanic Belt. *Earth-Science Rev.* 183, 153–181. doi:10.1016/j.earscirev.2016.12.006
- Gutierrez, Q. J., Escudero, C. R., and Núñez-Cornú, F. J. (2015). Geometry of the Rivera-Cocos Subduction Zone Inferred from Local Seismicity. *Bull. Seismological Soc. America* 105 (6), 3104–3113. doi:10.1785/0120140358
- Housh, T. B., Aranda-Gómez, J. J., and Luhr, J. F. (2010). Isla Isabel (Nayarit, México): Quaternary Alkaline Basalts with Mantle Xenoliths Erupted in the Mouth of the Gulf of California. *J. Volcanology Geothermal Res.* 197, 85–107. doi:10.1016/j.jvolgeores.2009.06.011
- Jaramillo, S. H., and Suárez, G. (2011). The December 4, 1948, Islas Marías, Mexico Earthquake (Mw 6.4): Reverse Faulting beneath the Tres Marías Escarpment

- and Implications for the Rivera-North American Relative Plate Motion. *Geophys. Int.* 50, 313–317. doi:10.22201/igeof.00167169p.2011.50.3.229
- Keen, C. E., Dickie, K., and Dafeo, L. T. (2018). Structural Characteristics of the Ocean-Continent Transition along the Rifted continental Margin, Offshore central Labrador. *Mar. Pet. Geology*, 89, 443–463. doi:10.1016/j.marpetgeo.2017.10.012
- Korenaga, J., Holbrook, W. S., Kent, G. M., Kelemen, P. B., Detrick, R. S., Larsen, H.-C., et al. (2000). Crustal Structure of the Southeast Greenland Margin from Joint Refraction and Reflection Seismic Tomography. *J. Geophys. Res.* 105 (B9), 21591–21614. doi:10.1029/2000JB900188
- Kostoglodov, V., and Bandy, W. (1995). Seismotectonic Constraints on the Convergence Rate between the Rivera and North American Plates. *J. Geophys. Res.* 100, 17977–17989. doi:10.1029/95JB01484
- Lizarralde, D., Axen, G. J., Brown, H. E., Fletcher, J. M., González-Fernández, A., Harding, A. J., et al. (2007). Variation in Styles of Rifting in the Gulf of California. *Nature* 448, 466–469. doi:10.1038/nature06035
- Lonsdale, P. (1989). "Geology and Tectonic History of the Gulf of California," in *The Eastern Pacific Ocean and Hawaii*. *Geol. Soc. Am.* Editors E. L. Winterer, D. M. Hussong, and R. W. Decker (Boulder, Colorado, N: The Geology of North America), 499–521.
- Luhr, J. F., and Carmichael, I. S. E. (1990). *Geology of the Volcán de Colima*, 107. Mexico City: Universidad Nacional Autónoma de México, Instituto de Geología, Boletín, 101.
- Luhr, J. F., Nelson, S. A., Allan, J. F., and Carmichael, I. S. E. (1985). Active Rifting in Southwestern Mexico: Manifestations of an Incipient Eastward Spreading-ridge Jump. *Geol.* 13, 54–57. doi:10.1130/0091-7613(1985)13<54:arismm>2.0.co;2
- Macías-Iñiguez, I., Yarbuh, I., Spelz-Madero, R., González-Fernández, A., Fletcher, J. M., Contreras, J., et al. (2019). Modo de extensión de la corteza y formación del Sistema Extensional de Cerralvo, sur del Golfo de California, a partir de datos de reflexión sísmica en 2D. *revmexg* 36, 334–347. doi:10.22201/cgeo.20072902e.2019.3.1352
- Madrigal, L. A., Núñez, D., Escalona-Alcázar, F. d. J., and Núñez-Cornú, F. J. (2021). Crustal Structure across the Northern Region of the Islas Mariás Archipelago. *Front. Earth Sci.* 9. doi:10.3389/feart.2021.682206
- Marín-Mesa, T., Núñez-Cornú, F. J., and Suárez-Plascencia, C. (2019). Analysis of the Seismicity in the Jalisco Block from June to December 2015. *Seism. Res. Lett.* 90, 1767–1778. doi:10.1785/0220190107
- Núñez-Cornú, F. J., Gutiérrez-Peña, Q. J., Escudero, C. R., and Córdoba, D. (2014). Imaging the Rivera and Cocos Plates below Jalisco and Michoacán Blocks from Seismicity Data. AGU Fall Meeting, San Francisco, California, 15–19 December 2014, Abstract T11C–4567.
- Núñez, D., Córdoba, D., Cotilla, M. O., and Pazos, A. (2016). Modeling the Crust and Upper Mantle in Northern Beata ridge (CARIBE NORTE Project). *Pure Appl. Geophys.* 173, 1639–1661. doi:10.1007/s00024-015-1180-0
- Núñez, D., Núñez-Cornú, F. J., Escalona-Alcázar, F. d. J., Córdoba, D., López Ortiz, J. Y., Carrillo de la Cruz, J. L., et al. (2019). Seismic Structure of the Southern Rivera Plate and Jalisco Block Subduction Zone. *Seismol. Res. Lett.* 90, 1756–1766. doi:10.1785/0220180399
- Núñez-Cornú, F. J., Córdoba, D., Dañoibeitia, J. J., Bandy, W. L., Figueroa, M. O., Bartolomé, R., et al. Tsujal Working Group (2016). Geophysical Studies across Rivera Plate and Jalisco Block, Mexico: Tsujal Project. *Seismological Res. Lett.* 87, 59–72. doi:10.1785/0220150144
- Núñez-Cornú, F. J., Sandoval, J. M., Alarcón, E., Gómez, A., Suárez-Plascencia, C., Núñez, D., et al. (2018). The Jalisco Seismic Accelerometric Telemetric Network (RESA). *Seismol. Res. Lett.* 89, 363–372. doi:10.1785/0220170157
- Núñez-Cornú, F. J., Escalona-Alcázar, F. d. J., Núñez, D., Trejo-Gómez, E., Suárez-Plascencia, C., and Rodríguez-Ayala, N. (2020). Study of Seismic Activity at Ceboruco Volcano (Nayarit, Mexico) in the Period 2012 to 2014. *J. South Am. Earth Sci.* 98, 102473. doi:10.1016/j.jsames.2019.102473
- Núñez-Cornú, F. J., Marta, R. L., Nava P, F. A., Reyes-Dávila, G., and Suárez-Plascencia, C. (2002). Characteristics of Seismicity in the Coast and north of Jalisco Block, Mexico. *Phys. Earth Planet. Interiors* 132, 141–155. doi:10.1016/s0031-9201(02)00049-3
- Núñez-Cornú, F. J., Reyes-Dávila, G. A., Lopez, M. R., Gomez, E. T., Camarena-García, M. A., and Ramírez-Vázquez, C. A. (2004). The 2003 Armeria, Mexico Earthquake (Mw 7.4): Mainshock and Early Aftershocks. *Seismological Res. Lett.* 75, 734–743. doi:10.1785/gssrl.75.6.734
- Ortega-Gutiérrez, F., and González-González, R. (1980). Nódulos de peridotita en la Isla Isabel, Nayarit. *Rev. Mex. Cienc. Geol.* 4, 82–83.
- Páramo, P., Holbrook, W. S., Brown, H. E., Lizarralde, D., Fletcher, J., Umhoefer, P., et al. (2008). Seismic Structure of the Southern Gulf of California from Los Cabos Block to the East Pacific Rise. *J. Geophys. Res.* 113, B03307. doi:10.1029/2007JB005113
- Pilia, S., Ali, M. Y., Searle, M. P., Watts, A. B., Lü, C., and Thompson, D. A. (2021). Crustal Structure of the UAE-Oman Mountain Range and Arabian Rifted Passive Margin: New Constraints from Active and Passive Seismic Methods. *J. Geophys. Res. Solid Earth* 126 (4), e2020JB021374. doi:10.1029/2020jb021374
- Pompa-Mera, V., Schaaf, P., Hernández-Treviño, T., Weber, B., Solís-Pichardo, G., Villanueva-Lascruaín, D., et al. (2013). Geology, Geochronology, and Geochemistry of Isla María Madre, Nayarit, Mexico. *Rev. Mex. Cienc. Geol.* 30, 1–23.
- Ruiz-Martínez, V. C., Badillo-Cruz, E. R., Escalona-Alcázar, F. J., Núñez-Cornú, F. J., and Córdoba-Barba, D. (2016). Registro magnético de la paleotectónica de los plutones de María Madre y Puerto Vallarta (Cretácico Superior, México). *Geo-Temas* 16, 885–888.
- Rutz López, M., Núñez Cornú, F. J., and Suárez Plascencia, C. (2013). Study of Seismic Clusters at Bahía de Banderas Region, Mexico. *Geofísica Internacional* 52, 59–72. doi:10.1016/s0016-7169(13)71462-4
- Rutz-López, M., and Núñez-Cornú, F. J. (2004). Sismotectónica del norte y oeste del bloque de Jalisco usando datos sísmicos regionales. *GEOS* 24, 2–13.
- Santibáñez-López, H. F. (2018). Imágenes Sísmicas en la Región Central de las Islas Mariás. Maestría en Ciencias en Geofísica. M.Sc. Thesis Mexico: Universidad de Guadalajara, Puerto Vallarta, 105. ((In Spanish)).
- Schaaf, P., Böhnell, H., Weber, B., Hernández-Treviño, T., Solís-Pichardo, G., Pompa-Mera, V., et al. (2015a). Magmatic Activity at Islas Mariás Archipelago: Key Events for Understanding Gulf of California Tectonics. 26th IUGG General Assembly. Prague, Czech Republic: Republic, VS-24. IAVCEI. IUGG-5302.
- Schaaf, P. E. G., Solís-Pichardo, G., Hernandez-Trevino, T., Villanueva, D., Arrieta, G. F., Rochin, H., et al. (2015b). Magmatic Activity at Islas Mariás Archipelago, Gulf of California: Oceanic Lithosphere with Gabbroic Sills versus Jurassic-Cretaceous Arc Components. Fall Meeting 2015. San Francisco (CA, USA). American Geophysical Union. Abstract Id V43B-3119.
- Sutherland, F. H., Kent, G. M., Harding, A. J., Umhoefer, P. J., Driscoll, N. W., Lizarralde, D., et al. (2012). Middle Miocene to Early Pliocene Oblique Extension in the Southern Gulf of California. 8, 752–770. doi:10.1130/GES00770.1
- Tinoco-Villa, M. E. (2015). Detección y Análisis de Enjambres Sísmicos en la Corteza Oceánica al Sur de las Islas Mariás Maestría en Ciencias en Geofísica. M.Sc. Thesis Mexico: Universidad de Guadalajara, Puerto Vallarta, 69. ((In Spanish)).
- Urias Espinosa, J., Bandy, W. L., Mortera Gutiérrez, C. A., Núñez Cornú, F. J., and Mitchell, N. C. (2016). Multibeam Bathymetric Survey of the Ipala Submarine Canyon, Jalisco, Mexico (20°N): The Southern Boundary of the Banderas Forearc Block? *Tectonophysics* 671, 249–263. doi:10.1016/j.tecto.2015.12.029
- Wessel, P., Luis, J. F., Uieda, L., Scharroo, R., Wobbe, F., Smith, W. H. F., et al. (2019). The Generic Mapping Tools Version 6. *Geochem. Geophys. Geosyst.* 20, 5556–5564. doi:10.1029/2019GC008515
- Wilson, D. S., and DeMets, C. (1998). Reply [to "Comment on "Relative Motions of the Pacific, Rivera, North American, and Cocos Plates since 0.78 Ma" by Charles DeMets and Douglas S. Wilson"]. *J. Geophys. Res.* 103, 24251–24256. doi:10.1029/98JB02127
- Yeats, R. S., Haq, B. U., Barron, J. A., Bukry, D., Crouch, J. K., Denham, C., et al. (1981). Initial Reports of the Deep Sea Drilling Project. *Initial Reports of the Deep Sea Drilling Project*, 63, 377–412. doi:10.2973/dsdp.proc.63.1981
- Zelt, C. A., and Smith, R. B. (1992). Seismic Traveltime Inversion for 2-D Crustal Velocity Structure. *Geophys. J. Int.* 108, 16–34. doi:10.1111/j.1365-246x.1992.tb00836.x

Conflict of Interest: The authors declare that the research was conducted in the absence of any commercial or financial relationships that could be construed as a potential conflict of interest.

Publisher's Note: All claims expressed in this article are solely those of the authors and do not necessarily represent those of their affiliated organizations, or those of the publisher, the editors and the reviewers. Any product that may be evaluated in this article, or claim that may be made by its manufacturer, is not guaranteed or endorsed by the publisher.

Copyright © 2021 Núñez, Acosta-Hernández, Escalona-Alcázar, Pilia, Núñez-Cornú and Córdoba. This is an open-access article distributed under the terms of the Creative Commons Attribution License (CC BY). The use, distribution or reproduction in other forums is permitted, provided the original author(s) and the copyright owner(s) are credited and that the original publication in this journal is cited, in accordance with accepted academic practice. No use, distribution or reproduction is permitted which does not comply with these terms.